J Appl Electrochem (2012) 42:153–162
DOI 10.1007/s10800-012-0382-8

ORIGINAL PAPER

Preparation, characterization, and application of alkaline leached Ni/Zn–Ni binary coatings for electro-oxidation of methanol in alkaline solution

Mir Ghasem Hosseini · Mehdi Abdolmaleki · Sajjad Ashrafpoor

Received: 8 November 2011 / Accepted: 20 January 2012 / Published online: 5 February 2012

Abstract The Ni–Zn binary coating was electrochemically deposited on a copper electrode. Then, it was etched in a concentrated alkaline solution (30 wt% NaOH) to obtain a porous electrocatalytic surface suitable for methanol electro-oxidation in alkaline solution. The surface compositions of coatings before and after alkaline leaching were determined by atomic absorption spectroscopy and energy dispersive X-ray analysis. The surface morphologies were investigated by scanning electron microscopy. It was found that the leached Ni–Zn coating has a porous structure. Electrocatalytic activity toward the methanol electro-oxidation was assessed by cyclic voltammetry and electrochemical impedance spectroscopy techniques. The activation of electrode related to the removal of existing corrosion products and formation of pores and cracks during alkaline leaching. Cyclic voltammetry studies confirmed that the alkaline leaching process improved the activity of Ni–Zn coating in comparison with smooth Ni deposit for the methanol electro-oxidation.

Keywords Leached Ni/Zn–Ni coating · Electrochemical deposition · Methanol electro-oxidation · Electrochemical impedance spectroscopy

1 Introduction

Fossil fuels constitute the major part of energy sources in the world today. Although they cause environment pollution and an irreversible effect on climate, they still continue to be the major energy sources for human activities. With the high energy consumption of the industrialized nations and increasing demand in developing countries and the rest of the world, the fossil fuel sources are fast approaching to an end, and the efforts of scientists to find alternative sources have never been this high previously [1–4]. An alternative energy source must qualify for certain criteria, such as transportation fuel, versatility, utilization efficiency, environmental compatibility, safety, and cost [5, 6]. Considering all these criteria, extensive studies have been devoted to the electrocatalytic oxidation of methanol which is of paramount importance in the development of direct methanol fuel cells [7, 8].

There is great deal of scientific and technological interest in the study of nickel electrode preparation, due to its application as cathodes of alkaline batteries [9–12], such as Ni–Cd, Ni–Fe, Ni–Zn alkaline batteries, and also its application in the organic electro-oxidation. In alkaline solutions, nickel can be easily converted to $Ni(OH)_2$ formed as α-$Ni(OH)_2$ and β-$Ni(OH)_2$ phases. At higher oxidation potentials, $Ni(OH)_2$ is further oxidized to β-NiOOH and γ-NiOOH, and, in basic medium, the Ni^{2+}/Ni^{3+} redox centers show high catalytic activity toward the oxidation of some small organic compounds. It was demonstrated by Kauler and Schagfer [13] that the $Ni(OH)_2$/NiOOH couple plays the key role in the electro-oxidation of organic compounds. This is because nickel oxyhydroxide was found to be a convenient and useful oxidizing agent for the oxidation of some small molecular alcohols into corresponding carboxylic acids [13–24].

In recent studies, Jafarian et al. [14] have reported the electro-catalytic oxidation of methanol on a Ni–Cu alloy electrode. Their results indicated that NiOOH, formed during anodic potential sweeping, showed high catalytic activity toward methanol oxidation. Zhang et al. [15] have

M. G. Hosseini (✉) · M. Abdolmaleki · S. Ashrafpoor
Electrochemistry Research Laboratory, Department of Physical Chemistry, Chemistry Faculty, University of Tabriz, Tabriz, Iran
e-mail: mg-hosseini@tabrizu.ac.ir

investigated the electrochemical characteristics of $Ni(OH)_2$ in a KOH solution containing aluminum hydroxide using galvanostatic charge–discharge, cyclic voltammetry, and electrochemical impedance spectroscopy methods (EIS). Nozad Golikand et al. [16] prepared a Nickel–PAN modified glassy-carbon electrode and studied its electrocatalytic activity toward methanol oxidation in alkaline solutions using cyclic voltammetry and amperometry methods.

For the first time, in this study, we prepared a porous Ni–Zn binary coating and used it for the electro-oxidation of methanol in alkaline solution. The catalytic activity of the electrodes toward the methanol electro-oxidation was tested by cyclic voltammetry and EIS.

2 Experimental

The copper electrodes were cut and mounted in polyester except for a surface area of 1 cm^2 for electrochemical measurements. Electrical connection was provided by a copper wire. Before electrodeposition, the electrode surfaces were polished with emery papers (up to 2,500 grit size), then washed with distilled water, thoroughly degreased in a 30 wt% NaOH solution for 5 min, washed again with distilled water, dipped into 10 wt% H_2SO_4 solution for 1 min followed by a rinse with distilled water and immersed in the bath solution. All the chemicals were of analytic grade purity and used as received. For each experiment, a freshly prepared electrode and solution were used. The chemical composition of plating bath and deposition conditions are given in Fig. 1. The surface of copper was coated with nickel and nickel (under layer)/zinc–nickel (top layer), and smooth Ni and Ni/Zn–Ni electrodes were obtained. After deposition, the electrodes were rinsed with distilled water to remove residues of bath chemicals and unattached particles. Ni/Zn–Ni electrode was immersed in 1 M NaOH for several hours until dissolution rate of Zn was slowed down, and then the electrode was exposed to 30 wt% NaOH solution at room temperature for 48 h until no more hydrogen bubbling was observed. These treatments promote a partial leaching of Zn producing a porous electrode of high surface area. After the leaching process, the working electrode was held at 100 mA cm^{-2} cathodic current density in 1 M KOH solution for 30 min to reduce the oxide film on the electrode surface as well as removal of corrosion products from the pores of coating and to obtain reproducible electrode surface characteristics [25].

In order to determine the loading amounts of smooth nickel electrode and Ni/Zn–Ni electrode before and after leaching, complete dissolution of the deposits in diluted HNO3 solution followed by atomic absorption spectroscopy analysis (AAS, NovAA 400-Analytikjena). Also, the surface composition of coatings before and after leaching was determined by energy dispersive X-ray (EDX) analysis. The scanning electron microscopy (SEM) images were taken using a SEM instrument (Philips, Model XL30).

The electrochemical studies captured were carried out in a conventional electrochemical cell. A standard three-electrode cell arrangement was used in all experiments. A platinum sheet of the geometric area of about 20 cm^2 was used as counter electrode, while all the potentials were measured with respect to a commercial saturated calomel

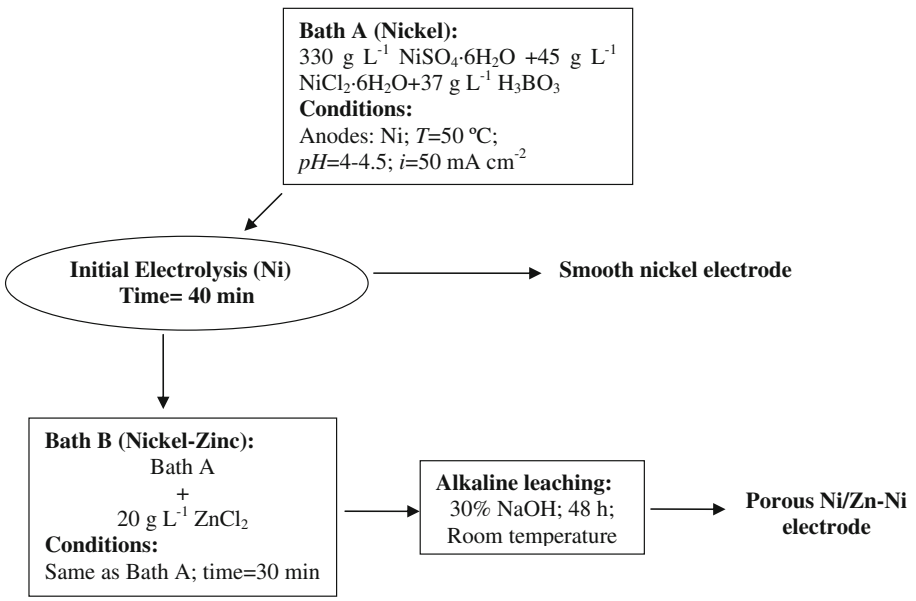

Fig. 1 Flowchart of the deposition methodology

electrode (SCE). Electrochemical experiments were carried out using a Princeton Applied Research, EG&G PARSTAT 2263 Advanced Electrochemical system run by PowerSuite software. The r.m.s amplitude of the modulation potential for the EIS measurements was 10 mV, and the frequency range was 100 kHz–10 mHz).

3 Results and discussion

3.1 Characterization of coatings

The SEM images in Fig. 2 show significant differences in morphology of the investigated coatings. Smooth Ni electrode shows a relatively homogeneous surface of small roughness, which can be considered as a quasi-two-dimensional surface (Fig. 2a). The surface SEM images of Ni/Zn–Ni electrode before and after leaching are shown in Fig. 2b, c, respectively. As seen from Fig. 2b, the deposit presents porous structure before leaching. Moreover, the porosity of surface is more and more improved; extra cracks and pores appeared after leaching of Zn from the deposit leading to a high surface area available for the methanol electro-oxidation (Fig. 2c).

The surface compositions of deposit before and after leaching were analyzed by EDX analysis. The EDX spectra obtained from the surface of coated electrodes are given in Fig. 3. The chemical composition of surface before leaching was 16.87 at.% Ni and 83.13 at.% Zn. After alkaline leaching, the surface composition changed to 62.07 at.% Ni and 37.93 at.% Zn. The results of composition AAS measurements were before leaching 17.27 at.% Ni and 82.73 at.% Zn and after alkaline leaching, the surface composition results changed as 67.47 at.% Ni and 32.53 at.% Zn. The results of composition of using AAS measurements were approximately in agreement the EDX measurements. The results of AAS and EDX analysis revealed that the Zn content decreased considerably after selective dissolution, which leads to pore-and-crack formation, yielding a highly porous surface suitable for use in methanol electro-oxidation.

3.2 Cyclic voltammetry

Figure 4 shows the cyclic voltammograms (CV) of a smooth nickel electrode and the porous Ni/Zn–Ni electrode in 1 M NaOH solution recorded at a potential sweep rate of 10 mV s^{-1}. It is observed that during the anodic sweeping, each electrode exhibited only one anodic peak at 0.38 and 0.49 V, respectively, and in the reverse sweeping, only one cathodic peak was detected, which was assigned to the redox process Ni^{2+}/Ni^{3+}. However, compared to what observed on the smooth nickel electrode (2.3 mA cm^{-2}), the current density on porous Ni/Zn–Ni electrode is higher

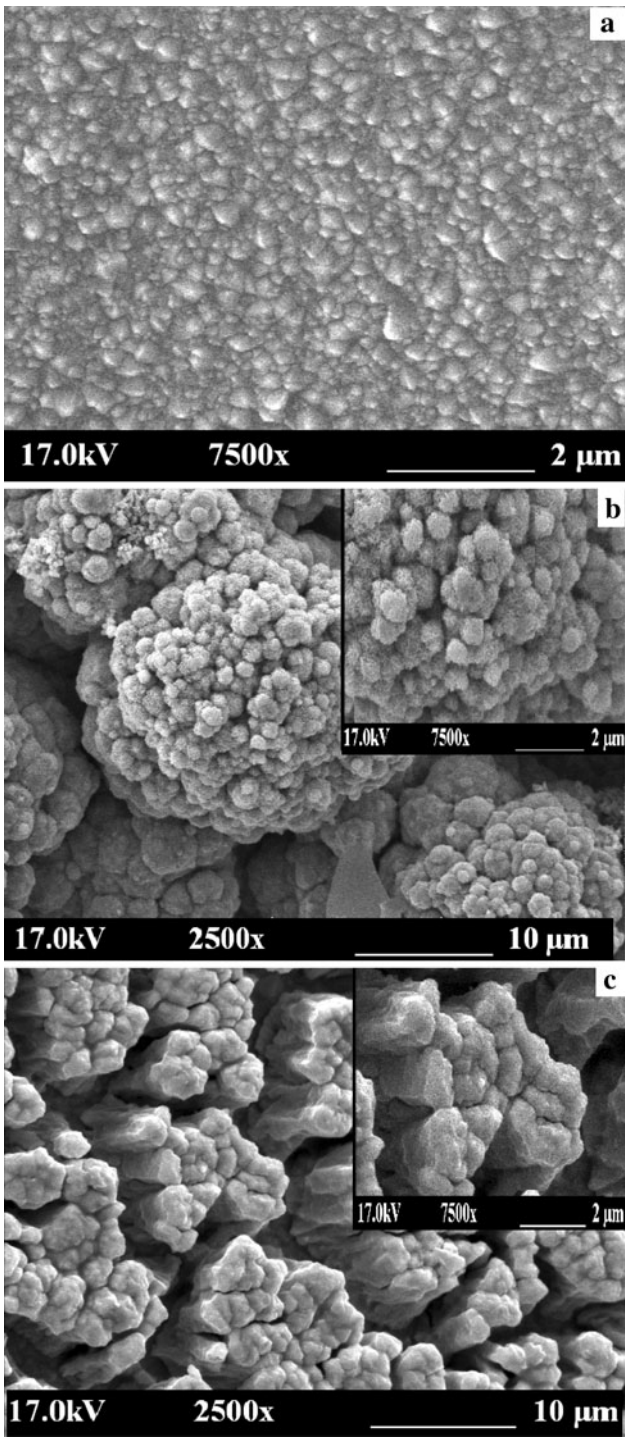

Fig. 2 SEM images of smooth nickel surface (**a**) and Ni/Zn–Ni surface before (**b**) and after (**c**) treatment with 30% NaOH solution

(50 mA cm^{-2}). This result can be attributed to the increase in the surface area and the change in surface features.

The electrocatalytic activity of leached Ni/Zn–Ni electrode for methanol oxidation was evaluated by cyclic voltammetry and compared to smooth nickel electrode. Figure 5 shows the CVs of electro-oxidation of methanol on smooth nickel and

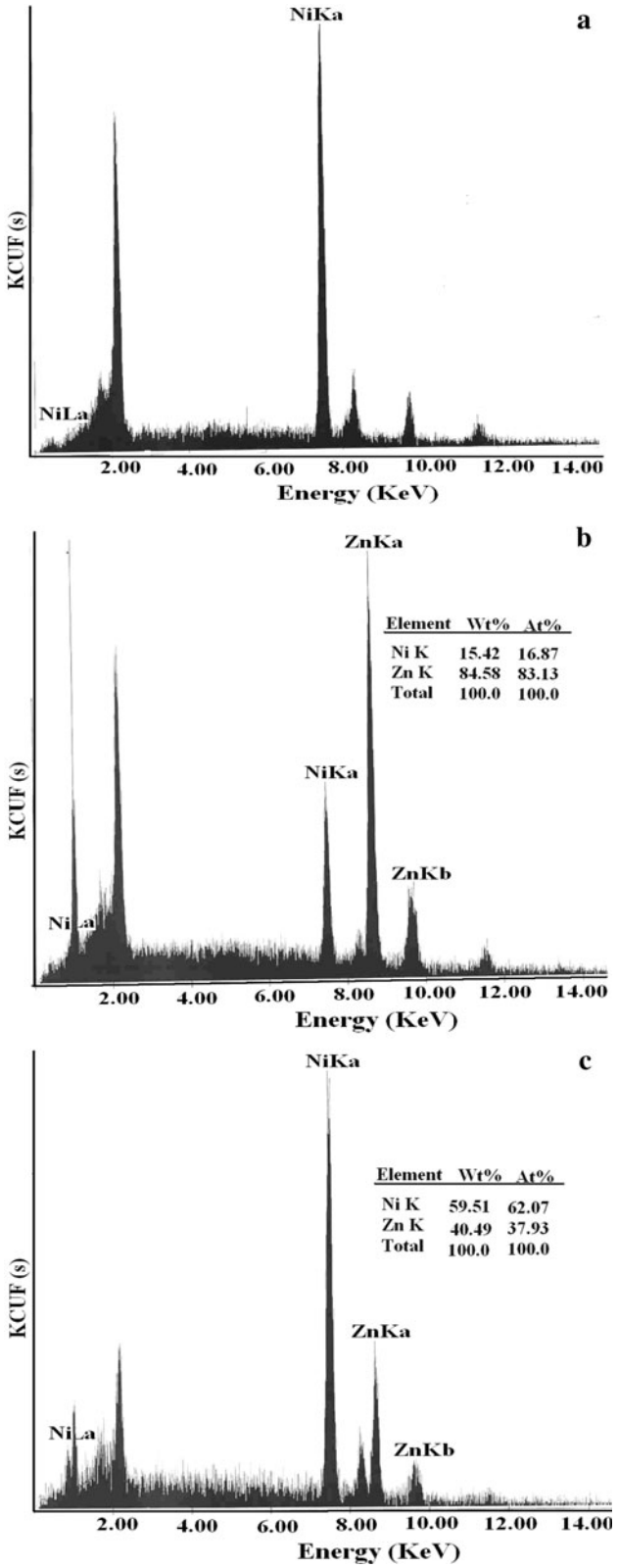

Fig. 3 EDX spectrums obtained from the surfaces of smooth nickel electrode (**a**) and Ni/Zn–Ni electrode before (**b**) and after (**c**) leaching

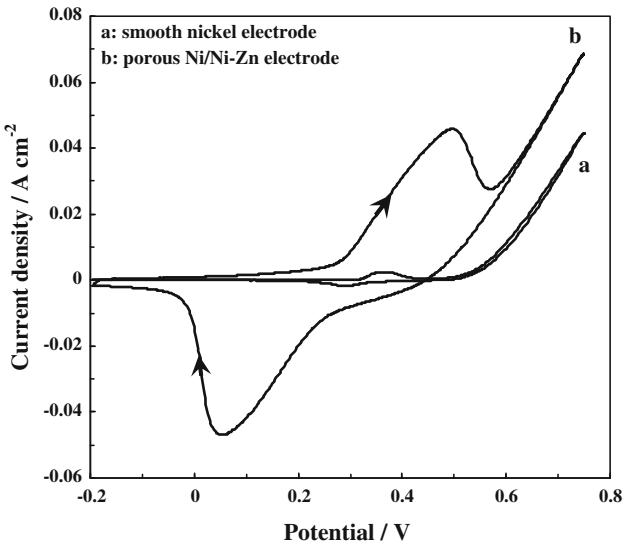

Fig. 4 Cyclic voltammograms of the smooth nickel electrode *a* and leached Ni/Zn–Ni electrode *b* in 1 M NaOH solution at a potential sweep rate of 10 mV s^{-1}

porous Ni/Zn–Ni electrodes in the presence and absence of methanol in 1 M NaOH solution at a potential sweep rate of 10 mV s^{-1}. An increment in the anodic peak current for peak (I) followed by the appearance of a new peak (II) at more positive potential are the main effects observed upon the addition 0.1 M methanol to the electrolyte. The peak I becomes a shoulder-peak and is hard to distinguish in the presence of methanol. Moreover, E_{paII} is higher than E_{paI}, probably implying that the active species needed for the methanol oxidation were mainly generated at higher anodic potentials. The appearance of the new anodic peak (II) leads to the conclusion that methanol oxidation takes place after the oxidation of $Ni(OH)_2$ to NiOOH [26, 27]. The phenomenon is similar to the smooth nickel electrode (Fig. 5a). The Ni^{2+}/Ni^{3+} redox couple acts as a catalyst for the oxidation of methanol in basic solutions. Therefore, for the Ni/Zn–Ni electrode peak, I is referred to the α-$Ni(OH)_2$/NiOOH redox couple, and another peak II was assigned to the methanol electro-oxidation. Furthermore, the current density of the Ni/Zn–Ni electrode is much higher than nickel electrode. For example, at the potential of peak II, the Ni/Zn–Ni electrode presents a current density of about 70 mA cm^{-2}, nearly 12 times higher than that of the nickel electrode (6 mA cm^{-2}) (see Fig. 5c). In addition, Fig. 5c shows that the onset oxidation potential of α-$Ni(OH)_2$/NiOOH redox couple on Ni/Zn–Ni electrode is lower than that on smooth nickel electrode. In general, the leached Ni/Zn–Ni electrode shows significantly greater electrocatalytic activity toward methanol oxidation than smooth nickel electrode. The high activity of leached Ni/Zn–Ni electrode can be related to the its high

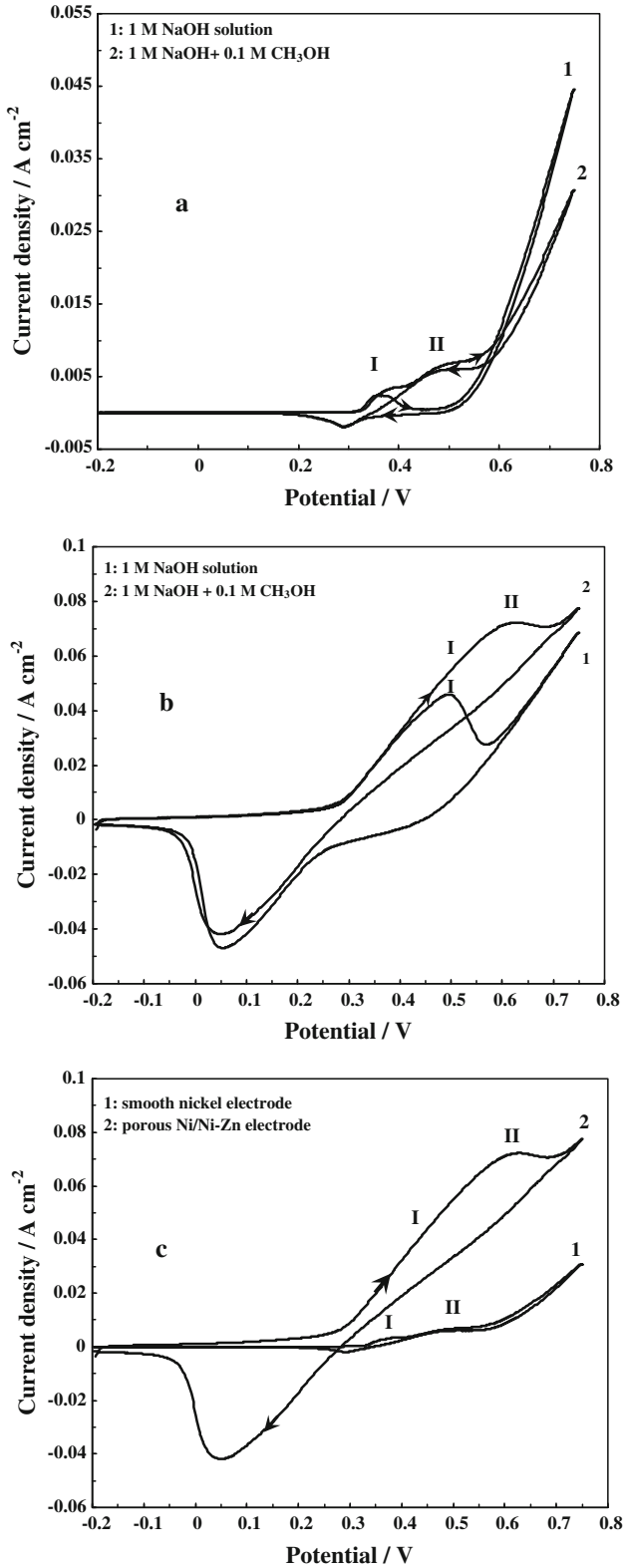

Fig. 5 Cyclic voltammograms (CVs) of smooth nickel electrode (**a**) and leached Ni/Zn-Ni electrode (**b**) in the absence *1* and the presence *2* of 0.1 M methanol in 1 M NaOH solution at a potential sweep rate of 10 mV s^{-1}. **c** Corresponding CVs of smooth nickel electrode *1* and leached Ni/Zn–Ni electrode *2* in 0.1 M methanol/1 M NaOH solution

surface area that was formed after selective dissolution of Zn from the surface as substantiated by SEM image (Fig. 2c).

Table 1 presents a comparison between peak current (i_p) of the methanol oxidation on leached Ni/Ni–Zn electrode and different electrodes in the literature [14, 16, 18, 24, 28–30]. It is evident from Table 1 that peak current density on leached Ni/Ni–Zn electrode is higher than that of the different electrode. In other words, among these electrodes, leached Ni/Ni–Zn electrode has the best electro-catalytic properties toward the methanol electro-oxidation in alkaline medium.

The influence of the scan rate on the cyclic voltammetry behavior of leached Ni/Zn–Ni electrode in 1 M NaOH/0.1 M methanol is shown in Fig. 6 which shows CVs of the leached Ni/Zn–Ni electrode from −0.2 to 0.75 V at different potential sweep rates from 2 to 80 mV s^{-1} in 1 M NaOH/0.1 M methanol solution. As the scan rate increases, the anodic peak potential shifts to more positive, and the cathodic peak potential is converted to a slightly negative direction. The plot of cyclic voltammetric peak currents I_{pa} against the square root of the voltage scan rate ($v^{1/2}$) gives a reasonable linear relationship ($R^2 = 0.9938$) (Fig. 7). In semi-infinite diffusion-controlled cyclic voltammetry in liquid electrolytes, I_{pa} against $v^{1/2}$ gives a linear relationship regardless of scan rate for a kinetically uncomplicated redox reaction. In this study, the linear relationship between I_{pa} and $v^{1/2}$ demonstrates that the electrochemical formation reaction of NiOOH from $Ni(OH)_2$ is a diffusion-controlled process.

It can be clearly seen from Fig. 6 that the current densities of cathodic peak (assigned to the reduction of Ni^{3+}/Ni^{2+}) increase with the scan rate. The increased cathodic current presumably results from increased reduction of the intermediates of the anodic peak during positive-sweep oxidation reactions. The phenomenon indicates that the electro-oxidation of nickel species to higher valence state is much faster than the catalytic oxidation of methanol. This reveals that the oxidation of methanol on leached Ni/Zn–Ni electrode may belong to a slow process. Thus, the rate-determining step for methanol oxidation is the reaction between the high oxidation state Ni^{3+} and methanol adsorbed on the surface of the leached Ni/Zn–Ni electrode.

Figure 8 shows the typical CVs of the Ni/Zn–Ni electrode from −0.2 to 0.75 V at the scan rate of 10 mV s^{-1} in 1 M NaOH solution with the concentration of methanol changed from 0.05 to 0.3 M. It is observed from Fig. 8 that as the methanol concentration increases, the current density of anodic peak II increases. This observation further indicates that the anodic peak II is contributed to the methanol electro-oxidation. It seems from Fig. 8 that only one anodic peak II appears in the presence of methanol. This is because the current density of anodic peak II is so large that the anodic peak I becomes ill-defined. In addition, Fig. 8 shows that the methanol oxidation peak potentials increase with increasing methanol concentration. It is suggested that

Table 1 The peak current density (i_p) of the methanol oxidation on leached Ni/Ni–Zn electrode and different electrodes

Electrode	Medium	Scan rate (mV s^{-1})	I_p (mA cm^{-2})	References
Ni–Cu	1 M NaOH + 0.5 M CH_3OH	10	1.5	[14]
Glassy carbon (GC) electrode modified with Ni(II)-1-(2-pyridylazo)-2-naphthol complex (Ni–PAN)	0.1 M NaOH + 0.1 M CH_3OH	20	0.44	[16]
Nickel dimethyglyoxime complex (NiDMG)	0.1 M NaOH + 0.1 M CH_3OH	20	0.3	[18]
$Ni/TiO_2/Ti$	0.5 M NaOH + 0.1 M CH_3OH	20	13.5	[24]
Ni/Ti	1 M KOH + 1 M CH_3OH	20	8	[28]
Nano Ni/Ti	1 M NaOH + 0.1 M CH_3OH	10	15	[29]
Ni	0.5 M Na_2SO_4 + 0.15 M NaOH + 1 M CH_3OH	10	7	[30]
Leached Ni/Zn–Ni	1 M NaOH + 0.1 M CH_3OH	10	70	This study

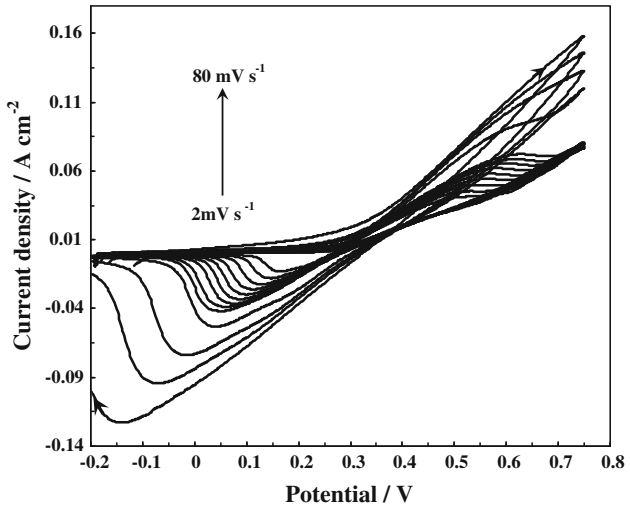

Fig. 6 Cyclic voltammograms obtained in 1 M NaOH + 0.1 M methanol for the leached Ni/Zn–Ni electrode in various scan rates

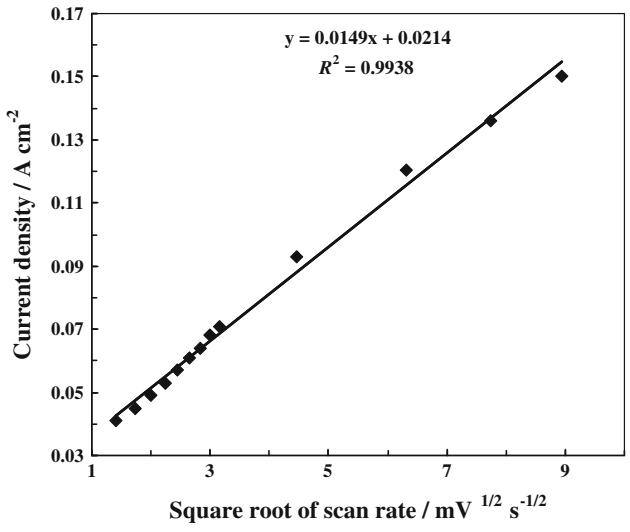

Fig. 7 The plot of variation of anodic current density with $\upsilon^{1/2}$ in 1 M NaOH + 0.1 M methanol for the leached Ni/Zn–Ni electrode

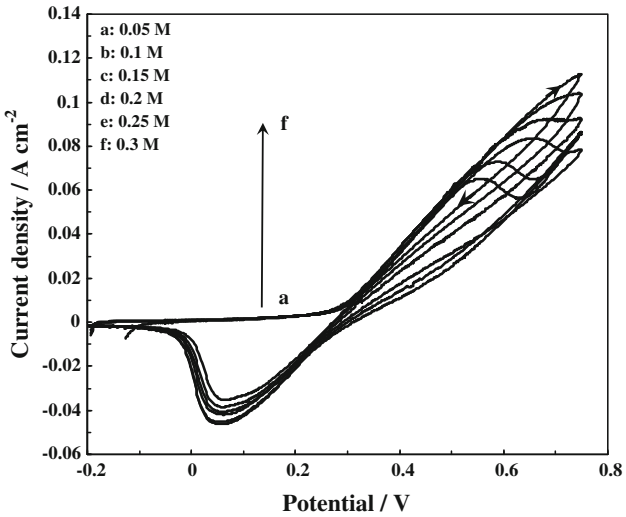

Fig. 8 Cyclic voltammograms of the leached Ni/Zn–Ni electrode from −0.2 to 0.75 V at the scan rate of 10 mV s^{-1} in 1 M NaOH solution with the various concentrations of methanol

the peak potential delay follows higher Ni^{2+} electron transfer resistance as methanol absorbs on the Ni^{2+} active center. Thus, higher methanol concentrations result in greater numbers of Ni^{2+} active centers covered by methanol. Subsequently, the potentials of peak II increase with methanol concentrations.

It can be seen from Fig. 9 that the current densities I_{pa} are well linearly proportional to the concentration of methanol. The linear dependence of I_{pa} upon the methanol concentrations allows us to suggest that the Ni/Zn–Ni electrode may be used as an amperometric sensor for methanol detection.

Temperature is one of the main factors affecting the reaction rate. In order to study electrocatalytic performance of Ni/Zn–Ni electrode on the electrolyte temperature, the temperature dependency of methanol oxidation on Ni/Zn–Ni electrode was investigated in the temperature range of 298–338 K by cyclic voltammetry method.

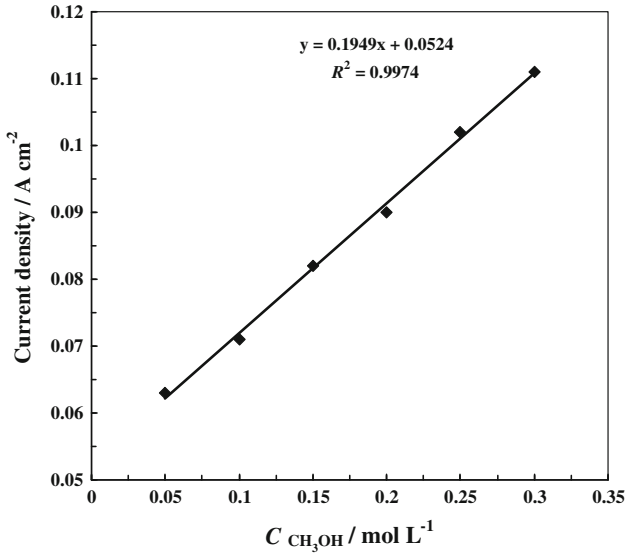

Fig. 9 Variations of anodic current density against methanol concentration for the leached Ni/Zn–Ni electrode

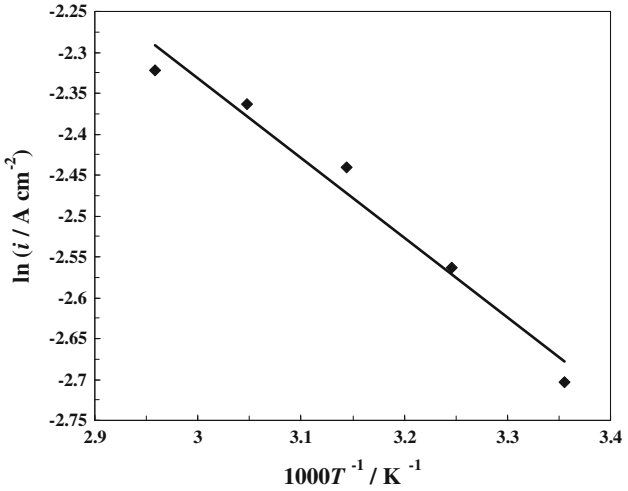

Fig. 11 Plot of ln i versus T^{-1} for the anodic current maximum for electro-oxidation of methanol

From Fig. 10, it can be seen that anodic current increase with temperature. Also as seen from Fig. 10, increase in temperature leads to a shift of anodic peak toward more negative potentials because of the more feasibility of oxidation at elevated temperatures. Figure 11 shows an Arrhenius plot of ln i versus T^{-1} for the Ni/Zn–Ni electrode. The apparent energy of activation was calculated from the slope of the plot and was found to be 8.2 kJ mol^{-1}. As the temperature increases, the electro-oxidation current density increases. This is attributed to the increase in the rate of charge transfer at electrode/electrolyte interface.

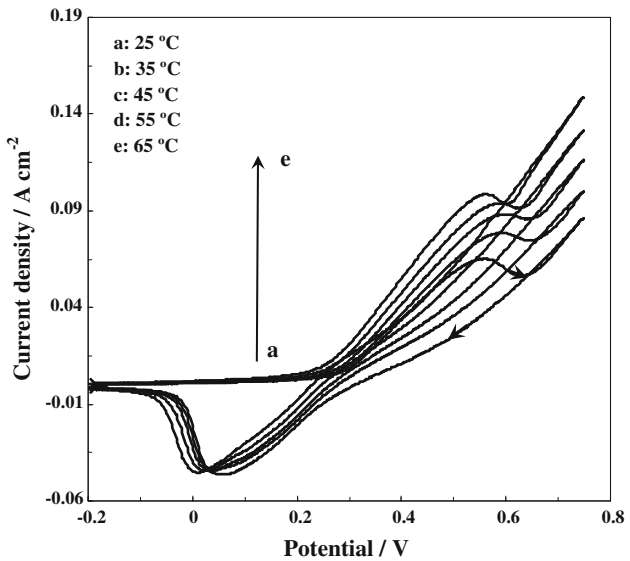

Fig. 10 The effect of temperature on cyclic voltammograms of methanol oxidation on leached Ni/Zn–Ni electrode in the range of 298–338 K in 1 M NaOH + 0.05 M methanol aqueous solution

3.3 Electrochemical impedance spectroscopy results

Figure 12 presents the equivalent circuits and Nyquist diagrams of leached Ni/Zn–Ni and smooth nickel electrodes recorded at anodic potential of 0.38 V, both in the absence methanol in 1 M NaOH solution. In order to fit impedance spectra obtained for the Ni/Zn–Ni electrodes, a two constant-phase elements (CPEs) serial model was applied (shown in the inset of the Nyquist diagram in Fig. 12). It consists of the solution resistance, R_s, in series with two parallel CPE-R elements (2-CPE model) [31, 32]. According to this model, the high-frequency time constant, independent of the potential, described by the R_p and CPE_p connected in parallel, is related to the electrode porosity, whereas the potential-dependent time constant is related to

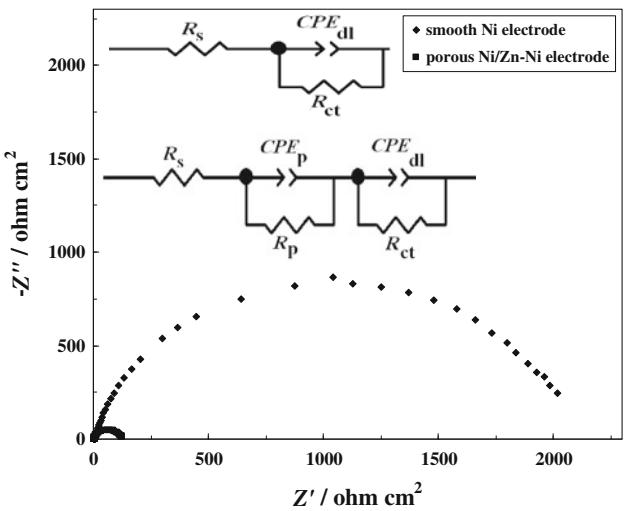

Fig. 12 Equivalent circuits and Nyquist diagrams of smooth nickel and leached Ni/Zn–Ni electrodes in 1 M NaOH solution at potential 0.38 V versus SCE

Table 2 Parameters obtained by fitting EIS results of Fig. 12

Electrode	R_s (Ω cm^2)	T_P (s^{Φ} Ω^{-1} cm^{-2})	R_P (Ω cm^2)	Φ_p	T_{dl} (s^{Φ} Ω^{-1} cm^{-2})	R_{ct} (Ω cm^2)	Φ_{dl}	C_{dl} (μF cm^{-2})	A_{real} (cm^2)	R_f
Smooth Ni	4.66	–	–	–	0.0003405	2090	0.86	119.2	5.959	5.959
Leached Ni/Zn–Ni	4.06	0.15	26.85	0.69	0.006858	103.5	0.914	5785	289.25	289.25

the kinetics of the electro-oxidation of methanol (R_{ct} and CPE_{dl} connected in parallel). The capacitance parameter T_{dl} is related to the average double layer capacitance C_{dl} by the relation:

$$C_{dl} = \left\{ T_{dl} / \left[\left(R_s + R_p \right)^{-1} + R_{ct}^{-1} \right]^{(1-\Phi)} \right\}^{1/\Phi}, \quad (1)$$

where Φ represents a factor of homogeneity [32]. In the case of smooth nickel electrode, the capacitance parameter T_{dl} is also related to the average double layer capacitance C_{dl} by a slightly different relation [32]:

$$C_{dl} = \left\{ T_{dl} / \left[R_s^{-1} + R_{ct}^{-1} \right]^{(1-\Phi)} \right\}^{1/\Phi}, \quad (2)$$

because the corresponding Nyquist diagrams exhibit only one semicircle. The model of the equivalent circuit includes the CPE in parallel with the charge transfer resistance R_{ct} (shown in the inset of the Nyquist diagram in Fig. 12). Taking that the average double layer capacitance (C_{dl}) of a smooth metal surface as 20 μF cm^{-2} [33, 34], the real surface area can be calculated as $A_{real} = C_{dl}/20$ (cm^2), and then the roughness factor, that characterizes the real-to-geometrical surface area ratio, can be calculated from $R_f = A_{real}/A_{geometric}$.

The mean values of the charge transfer resistance, double layer capacitance, true surface area, and roughness factor for the investigated electrodes are presented in Table 2. As seen from Table 2, smooth Ni electrode is the catalyst with the lowest true surface area and roughness factor values, while Ni/Zn–Ni electrode is the catalyst with the highest true surface area and roughness (compare to Fig. 2). Also, the lowest R_{ct}, 103.5 Ω cm^2, was observed on leached Ni/Zn–Ni electrode. This means that the catalytic activity of Ni/Zn–Ni electrode is higher than that of the smooth nickel electrode.

Figure 13 shows the equivalent circuits and Nyquist plots of the impedance of the Ni/Zn–Ni electrode for methanol electro-oxidation at different potentials in 1 M NaOH/0.1 M methanol solution.

Nyquist plots of presented in Fig. 13a suggest porosity of the electrode surfaces. Typically, Nyquist plots of porous electrodes show either a line with a slope of 45° or a semicircle at high frequencies followed by a semicircle at low frequencies [35–38].

In general, in Fig. 13a, two semi-circles could be detected on the Nyquist diagrams, indicating the presence

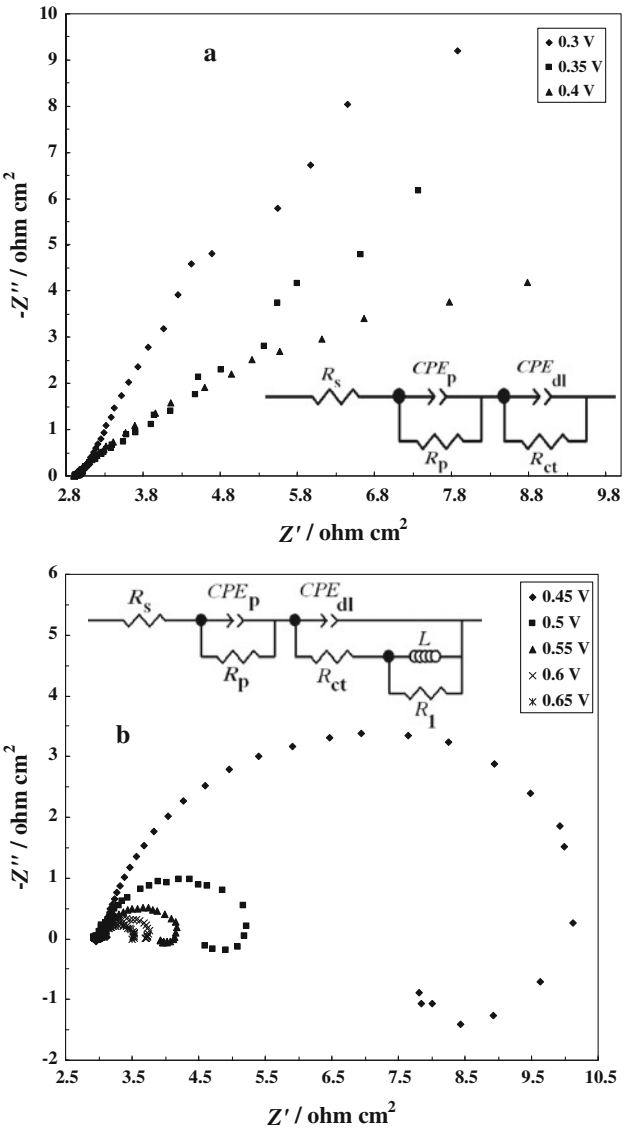

Fig. 13 Equivalent circuits and experimental Nyquist diagrams as a function of applied potential for methanol electro-oxidation on leached Ni/Zn–Ni electrode in 1 M NaOH + 0.1 M methanol aqueous solutions: **a** in potential 0.3, 0.35, 0.4 V versus SCE; **b** in potential 0.45, 0.5, 0.55, 0.6, 0.65 V versus SCE

of two time constants. The charge transfer resistance decreased with increasing potential indicating an increase in reaction kinetics at higher potentials.

In the potential between 0.45 and 0.65 V (Fig. 13b), the so-called pseudo-inductive behavior begins to emerge in the impedance plots, where two large positive loop at

Table 3 Equivalent circuit parameters of electro-oxidation of 0.1 M methanol on the leached Ni/Zn–Ni electrode in 1 M NaOH solution obtained from Fig. 13

Element	0.3 V	0.35 V	0.4 V	0.45 V	0.5 V	0.55 V	0.6 V	0.65 V
R_s (Ω cm^2)	2.94	2.88	2.92	2.402	2.916	2.96	2.98	2.99
T_P (s^{Φ} Ω^{-1} cm^{-2})	2.22	0.99	0.88	0.77	0.083	0.0056	0.002	0.0082
Φ_p	0.41	0.435	0.655	0.59	0.64	0.46	0.59	0.69
R_P (Ω cm^2)	2.908	2.7	2.28	0.602	0.087	0.017	0.0095	0.0215
T_{dl} (s^{Φ} Ω^{-1} cm^{-2})	0.68	1.587	1.578	0.511	0.48	0.518	0.577	0.498
Φ_{dl}	0.95	0.87	0.93	0.834	0.816	0.747	0.718	0.774
R_{ct} (Ω cm^2)	28.46	17.15	6.021	4.26	1.56	0.96	0.73	0.515
L (H)	–	–	–	86.46	7.29	1.42	0.43	0.14
R_1 (Ω cm^2)	–	–	–	4.97	1.09	0.663	0.363	0.108
Error (%)	1.63	4.57	3.414	2.32	1.98	1.77	1.36	2.11

higher frequency is accompanied by a small loop in the 4th quadrant at low frequency, with both diameters of the loops decreasing rapidly with the increase of the potential between 0.45 and 0.65 V as shown in Fig. 13b. An explanation for the occurrence of inductive behavior during methanol electro-oxidation can be attributed to the removal of adsorbed intermediates and creation of sites for further adsorption and reaction [28]. In general, the so-called pseudo-inductive behavior results from the 'relaxation phenomenon' between adsorption and dehydrogenation of methanol molecules and oxidation and adsorption of the CO-like species.

Table 3 shows the values of the equivalent circuit elements obtained by fitting the experimental results. Also the mean error of modulus is smaller than 5%, indicating a good fitting of the experimental data. In general, the presence of methanol speeds up the oxidation of $Ni(OH)_2$ into NiOOH because of the removal of the NiOOH by methanol, showing significantly high catalytic activity of the Ni/Zn–Ni toward the methanol oxidation.

According to Golikand et al. [17, 18], electrochemical oxidation of methanol at nickel electrodes is represented by

$$Ni(OH)_2 \rightarrow NiOOH + H^+ + e^- \quad (3)$$

$$NiOOH + CH_3OH \rightarrow Ni(OH)_2 + \text{oxidation products of methanol} \quad (4)$$

The active NiOOH formed during the positive potential scan is consumed through reaction (4). Subsequently, the formed $Ni(OH)_2$ in reaction (4) is again oxidized to NiOOH during the anodic potential sweep. This results in an increase in oxidation currents in the presence of methanol. In generally, the impedance data recorded at different potentials show evidence for two processes occurring at the interface: one is associated with the methanol electro-oxidation leading to the intermediates formation on the surface, and the other is assigned to the oxidation of intermediates. These observations are consistent with the results of CVs.

4 Conclusions

In this study, the smooth nickel and Ni/Zn–Ni electrocatalyst were prepared by electrodeposition methodology. Some of results can be detailed as follows: A nickel electrocatalyst with a high surface area was successfully prepared with a new electrodeposition methodology that allows the complete removal of Zn. The SEM results showed that the alkaline leaching process produces a highly porous catalytic surface suitable for use in electro-oxidation of methanol.

The results of cyclic voltammetric measurements and electrochemical impedance spectroscopy showed that the Ni/Zn–Ni electrode behaves as an efficient catalyst for the electro-oxidation of methanol in alkaline medium, and its electrocatalytic activity toward methanol oxidation is much higher than smooth nickel electrode. It was confirmed that during the anodic potential sweep, the electro-oxidation of methanol follows the formation of NiOOH on the electrode surface and is then catalyzed by NiOOH. The rate-determining step for methanol oxidation is the reaction between the high oxidation state nickel (Ni^{3+}) and the adsorbed methanol on the surface of the leached Ni/Zn–Ni electrode.

Acknowledgments The authors would like to acknowledge the financial support from the Office in Charge of Research of Iranian Nanotechnology Society and the financial support from the Office of Vice Chancellor in Charge of Research of University of Tabriz.

References

1. North DC (1992) Int J Hydrog Energy 17:509
2. Selvam P (1991) Int J Hydrog Energy 16:35

3. Barbir F, Veziroğlu TN, Plass HJ (1990) Int J Hydrog Energy 15:739
4. Lutfi N, Veziroğlu TN (1991) Int J Hydrog Energy 16:169
5. Bockris JO'M, Veziroğlu TN (1983) Int J Hydrog Energy 8:323
6. Veziroğlu TN, Barbir F (1992) Int J Hydrog Energy 17:391
7. Wasmus S, Kuver A (1999) J Electroanal Chem 461:14
8. Ren X, Zelenay P, Thomas S, Davey J, Gottesfeld S (2000) J Power Sources 86:111
9. Oliva P, Leonardi J, Laurent JF, Delmas C, Buaconnier JJ, Figlarz M, Fievent F, de Guibert A (1982) J Power Sources 8:229
10. Faure C, Delmas C, Fouassier M (1991) J Power Sources 35:279
11. Faure C, Borthomieu Y, Delmas C, Fouassier M (1991) J Power Sources 36:113
12. Freitas MBJG (2001) J Power Sources 93:163
13. Kauler J, Schaefer HJ (1982) Tetrahedron 38:3299
14. Jafrarian M, Moghaddam RB, Mahjani MG, Gobal F (2006) J Appl Electrochem 36:913
15. Zhang Q, Xu Y, Wang X (2004) Mater Chem Phys 86:293
16. Nozad Golikand A, Ghannadi Maragheh M, Irannejad L, Asgari M (2004) Russ J Electrochem 42:167
17. Abdel Rahim MA, Abdel Hameed RM, Khalil MW (2004) J Power Sources 134:160
18. Nozad Golikand A, Shahrokhian S, Asgari M, Ghannadi Maragheh M, Irannejad L, Khanchi A (2005) J Power Sources 144:21
19. Pournaghi-Azar MH, Nahalparvari H (2004) J Solid State Electrochem 8:550
20. Liu S-J (2004) Electrochim Acta 49:3235
21. Nozad Golikand A, Asgari M, Ghannadi Maragheh M, Shahrokhian S (2006) J Electroanal Chem 588:155
22. Wen TC, Lin SM, Tsai JM (1994) J Appl Electrochem 24:233
23. Lamy C, Belgsir EM, Leger J-M (2001) J Appl Electrochem 31:799
24. Hosseini MG, Momeni MM, Faraji M (2010) Electroanalysis 22:2620
25. Solmaza R, Döner A, Şahin İ, Yüce AO, Kardaş G, Yazıcı B, Erbil M (2009) Int J Hydrog Energy 34:7910
26. Vértes G, Horányi G (1974) J Electroanal Chem 52:47
27. Robertson PM (1980) J Electroanal Chem 111:97
28. Singh RN, Singh A, Anindita A, Mishra D (2008) Int J Hydrogen Energy 33:6878
29. Yi Q, Huang W, Zhang J, Liu X, Li L (2008) Catal Commun 9:2053
30. Gobal F, Valadbeigi Y, Kasmaee LM (2011) J Electroanal Chem 650:219
31. Birry L, Lasia A (2004) J Appl Electrochem 34:735
32. Kubisztal J, Budniok A, Lasia A (2007) Int J Hydrog Energy 32:1211
33. Chen L, Lasia A (1992) J Electrochem Soc 139:3214
34. Trasatti S, Petrii OA (1991) Pure Appl Chem 63:711
35. Hitz A, Lasia A (2001) J Electroanal Chem 500:213
36. Lasia A (1995) J Electroanal Chem 397:27
37. Lasia A (1997) J Electroanal Chem 428:155
38. Lasia A (2000) J Electroanal Chem 500:30